Chemical and Magnetic Interface Properties of Tunnel Junctions With Co_2MnSi/Co_2FeSi Multilayer Electrode Showing Large Tunneling Magnetoresistance

Jan Schmalhorst[1], Daniel Ebke[1], Marc D. Sacher[1], Ning-Ning Liu[1], Andy Thomas[1], Günter Reiss[1], Andreas Hütten[1,2], and Elke Arenholz[3]

[1]Thin Films and Nano Structures, Department of Physics, Bielefeld University, 33501 Bielefeld, Germany
[2]Institute for Nano-Technology, Research Center Karlsruhe, 76021 Karlsruhe, Germany
[3]Lawrence Berkeley National Laboratory, Berkeley, CA 94720 USA

Transport, as well as chemical and magnetic interface properties of two kinds of magnetic tunnel junctions (MTJs) with Co_2FeSi electrode, Al-O barrier, and Co-Fe counter electrode, are investigated. For junctions with Co_2FeSi single-layer electrodes, a tunnel magnetoresistance of up to 52% is found after optimal annealing for an optimal Al thickness of 1.5 nm, whereas the room temperature bulk magnetization of the Co_2FeSi film reaches only 75% of the expected value. By using a $[Co_2MnSi/Co_2FeSi]_{\times 10}$ multilayer electrode, the magnetoresistance can be increased to 114%, corresponding to a large spin polarization of 0.74, and the full bulk magnetization is reached. For Al thickness smaller than 1 nm, the TMR of both kinds of MTJs decreases rapidly to zero. On the other hand, for 2- to 3-nm-thick Al, the TMR decreases only slowly. The Al thickness dependence of the TMR is directly correlated to the element-specific magnetic moments of Fe and Co at the Co_2FeSi/Al-O interface for all Al thickness. Especially, for optimal Al thickness and annealing, the interfacial Fe moment of the single-layer electrode is about 20% smaller than for the multilayer electrode, indicating smaller atomic disorder at the barrier interface for the latter MTJ.

***Index Terms*—Heusler alloys, Heulser compounds, magnetic interface properties, magnetic tunneling junctions, X-ray absorption spectroscopy.**

MAGNETIC tunnel junctions (MTJs) consisting of ferromagnetic electrodes separated by a thin insulating tunnel barrier are basic elements for spintronic devices. A very large tunnel magnetoresistance (TMR) is anticipated. The TMR amplitude is connected to the Julliére spin polarization [1] $P_{a,b}$ of electrode a and b : $\mathrm{TMR} = 2P_aP_b/[1 - P_aP_b]$. Ferromagnetic half-metals—having a gap in the minority or majority electron density of states at the Fermi energy E_F and, thus, $P = 100\%$—are important to reach highest TMR amplitudes. This property has been predicted theoretically for some half and full Heusler compounds [2]–[5], such as Co_2MnSi and Co_2FeSi. The Heusler alloy Co_2FeSi crystallized in $L2_1$ structure has a magnetic moment of $6\mu_B$ per formula unit [5] and a very high Curie temperature of 1100 K [5], making it especially attractive for applications. MTJs with Co_2FeSi single-layer electrodes will be discussed first. It will be shown that the atomic ordering of the Co_2FeSi film is not perfect after optimal post-annealing resulting in reduced magnetization and spin polarization. To increase both properties, an improved atomic order of the Co_2FeSi is required. This can be achieved by introducing $[Co_2MnSi/Co_2FeSi]_{\times 10}$ multilayer electrodes instead of the Co_2FeSi single layers to force the atomic ordering of the Co_2FeSi layers by the adjacent Co_2MnSi layers.

DC- and RF-magnetron sputter deposition at RT from stoichiometric targets was used to prepare the MTJ stacks. On thermally oxidized Si(100) wafers we deposited a 40-nm-thick V buffer and subsequently a magnetically soft $Co_2FeSi^{100\ \mathrm{nm}}$ single layer or a $[Co_2MnSi^{5\ \mathrm{nm}}/Co_2FeSi^{5\ \mathrm{nm}}]_{\times 10}$ multilayer. This bottom electrode was coverd by a 0.5–3-nm-thick Al film and plasma oxidized for 150 s to form a tunnel barrier. This stack was *in situ* annealed at about 380 °C for 60 min. To remove surface contamination the barrier was oxidized for another 50 s after annealing and covered with the top electrode ($Co_{70}Fe_{30}{}^{5\ \mathrm{nm}}/Mn_{83}Ir_{17}{}^{10\ \mathrm{nm}}/Ta^{5\ \mathrm{nm}}/Cu^{50\ \mathrm{nm}}/Ta^{5\ \mathrm{nm}}/Au^{20\ \mathrm{nm}}$). Finally, the layer stacks were *ex situ* vacuum annealed at 275°C in a magnetic field of 0.1 T to set the exchange bias of the pinned electrode and patterned by optical lithography and ion beam etching. "Half" junctions without top electrode were also fabricated for X-ray absorption (XAS), X-ray magnetic circular dichroism (XMCD) and Auger depth profiling probing the structural and magnetic properties of the Heusler compound-based electrodes and at the Co_2FeSi/AlO_x interfaces. These "half" junctions were *ex situ* annealed up to 550°C. XAS and XMCD was performed at beamline 4.0.2 and 7.3.1.1 of the Advanced Light Source, Berkeley, CA. Surface-sensitive total electron yield (TEY) [6], as well as bulk-sensitive fluorescence yield (FY) spectra [6] were recorded.

Typical TMR majorloops (measured at low temperature) of our Co_2FeSi/AlO_x/Co-Fe junctions with optimum Al thickness of 1.5 nm are shown in Fig. 1(a): Using a Co_2FeSi single electrode a maximum TMR amplitude of 52% is found corresponding to $P_{\mathrm{Co2FeSi}} = 0.42$ (here, we assumed $P = 0.49$ for the Co-Fe electrode on top of the Al-O barrier [7]). The TMR amplitude of the optimal $[Co_2MnSi/Co_2FeSi]_{\times 10}/AlO_x$/Co-Fe junctions is more than two times larger than for the Co_2FeSi single-layer-based MTJ, namely 114% at 17 K. The according low temperature spin polarization of the $[Co_2MnSi/Co_2FeSi]_{\times 10}/AlO_x$ interface is 0.74, which is comparable to the highest values reported for Co_2MnSi-based junctions so far [8], [9]. The Al thickness

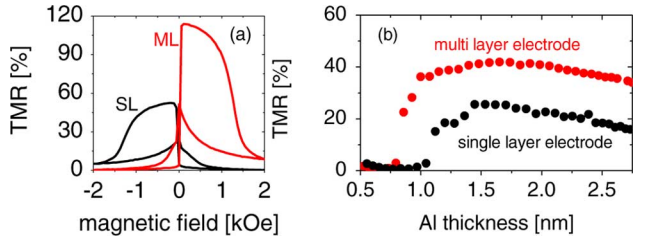

Fig. 1. (a) Low-temperature TMR majorloops of Co_2FeSi single-layer ("SL" black curve, 16 K) and $[Co_2MnSi/Co_2FeSi]_{\times 10}$ multilayer ("ML" red curve, 17 K)-based MTJs measured with 10-mV bias for 1.5-nm-thick Al. (b) Room-temperature TMR amplitude (10-mV bias) of MTJs with Co_2FeSi single and $[Co_2MnSi/Co_2FeSi]_{\times 10}$ multilayer electrode as a function of Al thickness.

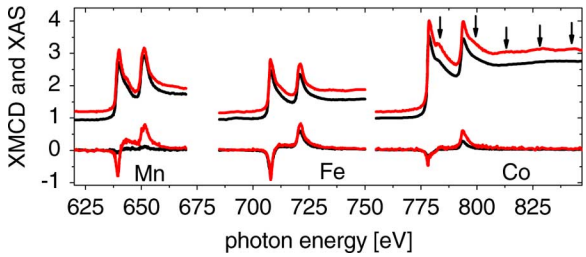

Fig. 2. Bulk sensitive XAS and XMCD spectra (taken in FY mode) at the Mn-, Fe-, and Co-$L_{2,3}$ edge for as prepared (black line) and annealed (400 °C, red line) $[Co_2MnSi/Co_2FeSi]_{\times 10}$ multilayer-based half junctions (1.5 nm Al).

dependence of the TMR, measured at room temperature is shown in Fig. 1(b). For Al thinner than 1 nm prior to oxidation the TMR drops rapidly, for Al thicker than the optimal value of about 1.5 nm a slow decrease is observed (this has also been found for standard MTJs with Ni-Fe/Co-Fe electrodes). As found previously for Co_2MnSi-based junctions [10], the Co_2FeSi single layer and the $[Co_2MnSi/Co_2FeSi]_{\times 10}$ multilayer are (110)-textured, the lattice parameter is 5.65 Å. The room temperature magnetization of the $Co_2FeSi^{100\ nm}$ single film increases from (543 ± 42) kA/m in the as prepared state to maximal (901 ± 114) kA/m after annealing at 400 °C. This is smaller than the bulk magnetization of $L2_1$-ordered Co_2FeSi of 1241 kA/m [5] and hints at residual disorder in the film even after annealing. For higher annealing temperatures, the bulk magnetization falls below the value in the as prepared state, which is related to diffusion of V (see below). In contrast the magnetization of the $[Co_2MnSi^{5\ nm}/Co_2FeSi^{5\ nm}]_{\times 10}$ multilayer electrode increases from (432 ± 23) kA/m in the as prepared state to (1151 ± 101) kA/m after annealing at 400 °C. Within the experimental error, this is in accordance with the mean magnetization of the multilayer (1134 kA/m) assumed to be the weighted average of bulk magnetizations of Co_2FeSi (1241 kA/m) and Co_2MnSi (1026 kA/m [4]). This suggests that the multilayer structure supports the thermally induced ordering of the Co_2FeSi. The bulk sensitive XAS and XMCD of the multilayer system do not depend on the Al thickness, in the as prepared state only Co and Fe contribute significantly to the magnetization of the multilayer (Fig. 2). EXAFS oscillations indicating atomic ordering of the Heusler film after annealing at 400 °C and shoulders at about 4 eV above the maximum intensities of the resonances (for Co, these features are marked by arrows in Fig. 2) reflecting small peaks in the density of

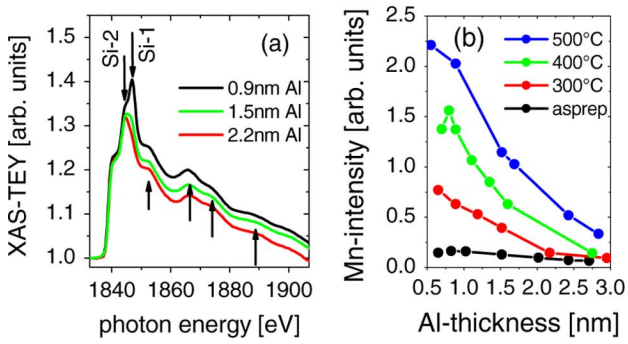

Fig. 3. (a) Surface sensitive XAS spectra at Si-K edge for an annealed (400 °C) $[Co_2MnSi/Co_2FeSi]_{\times 10}$ multilayer-based half junction with different Al thickness. Si-1 corresponds to interfacial SiO_2, Si-2 to a small peak in the $2p$ density of states of the Heusler alloy. The EXAFS oscillations marked by black arrows indicate atomic ordering of the alloy. (b) Maximal XAS intensity at Mn-L_3 edge for different annealing temperatures as a function of Al thickness. This indicates Mn diffusion to the barrier.

unoccupied d-like states are found after optimal annealing. Simultaneously, the XMCD asymmetries of all components increases, especialy for Mn. Auger depth profiling was used to investigate the diffusion processes within the stacks. The multilayer structure was essentially conserved after annealing up to 400°C, but Mn diffusion to the lower barrier interface already occured at 300 °C and became stronger with higher temperature and smaller Al thickness as indicated by the Mn intensities found by surface sensistive XAS on "half" junctions [Fig. 3(b)]. The XAS spectra showed, that the Mn diffused to the lower barrier interface is oxidized to MnO. Furthermore, some SiO_2 was found at the lower barrier interface even for optimal Al thickness of 1.5 nm [Fig. 3(a)]. As for MnO, the SiO_2 concentration increases with decreasing Al thickness. Because MnO is paramagnetic at RT, the XMCD signal at the Mn-$L_{2,3}$ edge correspondingly decreases to the increased MnO concentration at the interface [Fig. 4(c)]. Co and Fe showed typical metallic absorption spectra at the interface for $d_{Al} \geq 1$nm. For $d_{Al} < 1$nm, FeO_x was formed at the interface and the interfacial Fe and Co magnetic moments were reduced even after annealing [Fig. 4(a) and (b)]. After optimal annealing around 400 °C, the thickness dependence of the Fe and Co magnetic moment is similar to the TMR amplitude: the highest TMR is found, when the interfacial Fe and Co magnetic moments are maximum. Compared to the interfacial magnetic moments of Co_2FeSi single-layer-based MTJs, the normalized XMCD asymmetry (and accordingly the magnetic moment) of the $[Co_2MnSi/Co_2FeSi]_{\times 10}$ multilayer-based half junction is comparable for Co but significantly larger for Fe. This behavior is correlated to the bulk magnetization of both stacks discussed above and hints again at higher atomic disorder and, accordingly, makes the smaller TMR amplitude of the Co_2FeSi single-layer-based MTJs reasonable. The element-specific interfacial magnetic moments $m^{Co,Fe,Mn}$ of the optimized $[Co_2MnSi/Co_2FeSi]_{\times 10}$ multilayer-based half junction ($d_{Al} = 1.5$ nm, annealed at 400 °C) are close to the values expected from theory: We found interfacial element-specific magnetic moments (measured at 20 K) per number of 3 d-holes n_d of $0.69\mu_B$ for Co, $1.05\mu_B$ for Fe, and $0.82\mu_B$ for Mn by using XMCD sum rules [11]. By taking

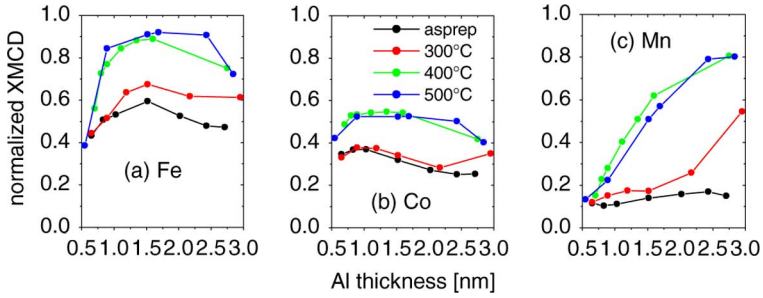

Fig. 4. XMCD asymmetry measured in surface sensitive TEY mode normalized to the maximal intensity at the L_3 edges of (a) Fe, (b) Co, and (c) Mn (this quantity is proportional to their interfacial magnetic moment) for $[Co_2MnSi/Co_2FeSi]_{\times 10}$ multilayer-based "half" junctions as a function of Al thickness and annealing temperature.

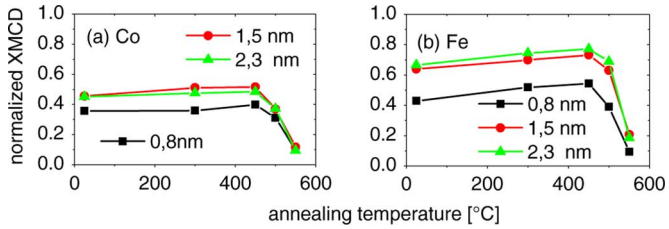

Fig. 5. XMCD asymmetry measured in surface sensitive TEY mode normalized to the maximal intensity at the L_3 edges of (a) Co and (b) Fe for Co_2FeSi single-layer-based half junctions as a function of Al thickness and annealing temperature.

n_d from band structure calculations into account (Co_2MnSi [12]: $n_d^{Co} = 2.24$, $n_d^{Mn} = 4.52$; Co_2FeSi [13]: $n_d^{Co} = 2.28$, $n_d^{Fe} = 3.48$) this corresponds to magnetic moment ratios of $m^{Mn}/m^{Co} = 2.4$ (the theoretical value for Co_2MnSi is 2.9 [12]) and $m^{Fe}/m^{Co} = 2.3$ (the theoretical value for Co_2FeSi is 2.1 [13]). Especially, the reduced m^{Mn}/m^{Co} ratio is reasonable because of the interfacial MnO, which is not ferromagnetically ordered. After annealing above 450 °C V diffused into the Co_2FeSi single-layer electrode and towards the barrier. This seems to be responsible for the strong reduction of its bulk magnetic moment. Although the full bulk magnetization of the $[Co_2MnSi/Co_2FeSi]_{\times 10}$ multilayer-based MTJs is reached after optimal annealing, its spin polarization is still not 100%. This hints at residual structural imperfections at the multilayer - barrier interface, e.g., as mentioned above MnO and SiO_2 was formed at the interface hindering perfect atomic ordering of the Co_2FeSi at the interface. As for our MTJs with Co_2MnSi single-layer electrode [14], where interfacial MnO and SiO_2 was identified by X-ray absorption spectroscopy, too, these imperfections can reduce the effective spin polarization of the multilayer barrier interface by spin flip scattering on MnO, unpolarized conductance via defect states in the barrier and residual disorder close to the barrier leading to additional states in the theoretically predicted minority electrons gap around E_F.

In summary, the full Heusler compound Co_2FeSi has been integrated into magnetic tunnel junctions with Al-O barrier and Co-Fe counter electrode. By using $[Co_2MnSi/Co_2FeSi]_{\times 10}$ multilayer electrodes, the atomic ordering of the Co_2FeSi could be improved compared to the Co_2FeSi single layers. The resulting bulk magnetization of the multilayers reached the expected value. For optimal Al thickness of 1.5 nm, the Fe magnetic moment at the Co_2FeSi/Al-O interface was significantly larger than for the Co_2FeSi single layer and a maximum effective spin polarization of 0.74 has been reached. For smaller and larger Al thickness, the interfacial magnetic moments showed a similar behavior as the TMR amplitude.

Acknowledgment

This work was supported by the Deutsche Forschungsgemeinschaft (DFG). The authors would like to thank A. Scholl and A. Doran for their valuable help during beamtime at BL 7.3.1.1. The Advanced Light Source is supported by the U.S. Department of Energy under Contract No. DE-AC02-05CH11231.

References

[1] M. Julliere, *Phys. Lett.*, vol. 54A, p. 225, 1975.
[2] R. de Groot, F. Mueller, P. van Engen, and K. Buschow, *Phys. Rev. Lett.*, vol. 50, p. 2024, 1983.
[3] S. Ishida, T. Masaki, S. Fujii, and S. Asano, *Phys. B*, vol. 245, p. 1, 1998.
[4] I. Galanakis, P. H. Dederichs, and N. Papanikolaou, *Phys. Rev. B*, vol. 66, p. 174429, 2002.
[5] S. Wurmehl, G. Fecher, H. C. Kandpal, V. Ksenofontov, C. Felser, H.-J. Lin, and J. Morais, *Phys. Rev. B*, vol. 72, p. 184434, 2005.
[6] Y. U. Idzerda, C. T. Chen, H.-J. Lin, G. Meigs, G. H. Ho, and C.-C. Kao, *Nucl. Instrum. Meth. Phys. Res. A*, vol. 347, p. 134, 1994.
[7] A. Thomas, Ph.D. dissertation, Univ. Bielefeld, Bielefeld, Germany, 2004.
[8] J. Schmalhorst, S. Kämmerer, G. Reiss, and A. Hütten, *Appl. Phys. Lett.*, vol. 86, p. 052501, 2005.
[9] M. Oogane, Y. Sakuraba, J. Nakata, H. Kubota, Y. Ando, A. Sakuma, and T. Miyazaki, *J. Phys. D: Appl. Phys.*, vol. 39, p. 834, 2006.
[10] S. Kämmerer, S. Heitmann, D. Meyners, D. Sudfeld, A. Thomas, A. Hütten, and G. Reiss, *J. Appl. Phys.*, vol. 93, p. 7945, 2003.
[11] C. T. Chen, Y. U. Idzerda, H.-J. Lin, N. V. Smith, G. Meigs, E. Chaban, G. H. Ho, E. Pellegrin, and F. Sette, *Phys. Rev. Lett.*, vol. 75, p. 152, 1995.
[12] J. Schmalhorst, S. Kämmerer, M. Sacher, G. Reiss, A. Hütten, and A. Scholl, *Phys. Rev. B*, vol. 70, p. 024426, 2004.
[13] G. Fecher, private communication.
[14] J. Schmalhorst, A. Thomas, S. Kämmerer, O. Schebaum, M. D. Sacher, G. Reiss, A. Hütten, A. Turchanin, A. Gölzhäuser, and E. Arenholz, *Phys. Rev. B*, vol. 75, p. 014403, 2007.